^{18}F-4FMFES and ^{18}F-FDG PET/CT in Estrogen Receptor–Positive Endometrial Carcinomas: Preliminary Report

Michel Paquette[1], Esteban Espinosa-Bentancourt[1], Éric Lavallée[1], Serge Phoenix[1], Korine Lapointe-Milot[2], Paul Bessette[2], Brigitte Guérin[1], and Éric E. Turcotte[1]

[1]*Department of Nuclear Medicine and Radiobiology, Université de Sherbrooke, Sherbrooke, Québec, Canada; and* [2]*Department of Obstetrics and Gynecology, Université de Sherbrooke, Sherbrooke, Québec, Canada*

See an invited perspective on this article on page 700.

This article reports the preliminary results of a phase II clinical trial investigating the use of the estrogen receptor (ER)–targeting PET tracer 4-fluoro-11β-methoxy-16α-^{18}F-fluoroestradiol (^{18}F-4FMFES) and ^{18}F-FDG PET in endometrial cancers. In parallel, noninvasive interventions were attempted to slow progression of ^{18}F-4FMFES metabolites in the intestines to reduce abdominal background uptake. **Methods:** In an ongoing study, 25 patients who received prior pathologic confirmation of an ER-positive endometrial cancer or endometrial intraepithelial neoplasia agreed to participate in the ongoing clinical trial. Patients were scheduled for ^{18}F-FDG and ^{18}F-4FMFES PET/CT imaging in random order and within 2 wk. Patients were administered either 4 mg of loperamide orally before ^{18}F-4FMFES tracer injection or repeated intravenous injection of 20 mg of hyoscine *N*-butylbromide during ^{18}F-4FMFES PET/CT. Regions of interest covering the whole abdomen and excluding the liver, bladder, and uterus were drawn for the ^{18}F-4FMFES PET images, and an SUV threshold of more than 4 was applied. The volume of the resulting region was compared between the different interventions to estimate the extent of the intestinal background uptake. **Results:** Repeated injection of hyoscine *N*-butylbromide substantially reduced the intestinal background volume, whereas loperamide had a significant but moderate effect. ^{18}F-4FMFES tumor SUV_{max} ranged from 3.0 to 14.4 (9.4 ± 3.2), whereas ^{18}F-FDG SUV_{max} ranged from 0 to 22.0 (7.5 ± 5.1). Tumor-to-background ratio was significantly higher for ^{18}F-4FMFES (16.4 ± 5.4) than for ^{18}F-FDG (7.4 ± 4.6). Significant differences were observed between grade 1 and higher-grade tumors concerning ^{18}F-4FMFES uptake and contrast, ^{18}F-FDG uptake, and the ^{18}F-FDG/^{18}F-4FMFES uptake ratio. **Conclusion:** It is possible to improve ^{18}F-4FMFES abdominal background using hyoscine *N*-butylbromide. Both ^{18}F-FDG and ^{18}F-4FMFES PET are suitable for detection of ER-positive endometrial cancers, although ^{18}F-4FMFES yielded a better tumor contrast than did ^{18}F-FDG.

Key Words: endometrial carcinoma; ^{18}F-4FMFES; abdominal background

J Nucl Med 2022; 63:702–707
DOI: 10.2967/jnumed.121.262617

Endometrial cancers affected 382,069 women worldwide in 2018, and 89,929 died from the disease (*1*). About two thirds of endometrial cancers are diagnosed at an early, localized stage, for which prognosis is very favorable. The estrogen receptor (ER) is expressed in nearly 80% of uterine tumors (*2*), a patient subset that has an improved 5-y disease-free survival compared with ER-negative disease (*3,4*). Moreover, the success rate of adjuvant hormone therapies was shown to be dependent on ER status for endometrial cancers (*5,6*). As such, knowledge of ER status is increasingly evidenced to be crucial for this disease, both for prognosis and for therapy management.

Current diagnostic tools for endometrial cancers include transvaginal echography, CT, and MRI (*7*). More recently, the use of ^{18}F-FDG PET imaging has been spreading and has contributed to the detection and staging of those cancers (*8,9*). However, ^{18}F-FDG indicates only the relative avidity of tissues and tumors for glucose and as such is prone to false-negatives (hypometabolic tumors) and false-positives such as inflammation and physiologic uptake (*10,11*). As such, even if it supplements anatomic imaging such as CT and MRI, ^{18}F-FDG PET has a sensitivity and specificity ranging from poor to moderate for endometrial cancers (*8*).

To improve imaging of endometrial cancers and at the same time allow noninvasive assessment of ER status, a few groups have explored the use of the estrogenlike ^{18}F-16α-fluoroestradiol (^{18}F-FES) PET tracer in the clinical setting. ^{18}F-FES tumor uptake was shown to correlate well with the biopsy-determined ER status in endometrial cancers (*12,13*). The successive use of ^{18}F-FDG PET and ^{18}F-FES PET enabled discrimination between low- and high-grade endometrial carcinomas (*14*). The ^{18}F-FDG/^{18}F-FES tumor uptake ratio also correlated well with progression-free and overall survival in uterine sarcomas (*15,16*).

More recently, ^{18}F-FES PET was shown in a prospective study to be better than ^{18}F-FDG PET in evaluating endometrial cancer patient outcome, further displaying the potential of ER imaging for this disease (*17*). Despite those successes, ^{18}F-FES PET has some shortcomings, including slow blood clearance and rapid metabolization (*18,19*), both of which are factors increasing nonspecific signal and hence reducing tumor detectability.

To palliate the main weaknesses of ^{18}F-FES, our group developed an alternative ER-targeting molecule, 4-fluoro-11β-methoxy-16α-^{18}F-fluoroestradiol (^{18}F-4FMFES) (*20,21*), that was shown to resist hepatic metabolism in humans. Its very low binding to plasma globulins resulted in a 5-fold reduction of tracer in the blood pool in the clinical setting

Received May 20, 2021; revision accepted Aug. 11, 2021.
For correspondence or reprints, contact Éric E. Turcotte (eric.e.turcotte@usherbrooke.ca).
Published online Aug. 19, 2021.

(*22,23*). Combined, those 2 factors substantially reduced ^{18}F-4FMFES accumulation in nonspecific organs, compared with ^{18}F-FES, resulting in a much lower background signal (*23*). Consequently, ^{18}F-4FMFES generated a significantly better tumor contrast than did ^{18}F-FES in a phase II clinical study on a breast cancer cohort, allowing detection of more ER-positive (ER+) tumors than was previously possible (*23*). Preliminary reports indicated that ^{18}F-4FMFES complements standard ^{18}F-FDG PET imaging in breast cancer patients (*24*).

The recent success of ^{18}F-4FMFES PET in ER+ breast cancers in the clinical setting foretells its usability for ER+ endometrial cancers as well. Given the high prevalence of ER (*2*) and the importance of ER status (*3,4*) in endometrial cancers, this novel ER-targeting PET imaging modality might improve the diagnostic determination and the noninvasive ER status determination of those cancers. ^{18}F-FDG tumor uptake was shown to follow an inverse relationship with ER expression in breast cancers (*25,26*), and combined ^{18}F-FDG and ^{18}F-FES PET was shown superior to each tracer alone in breast cancers (*27*) and endometrial cancers (*14,15*). As such, the ^{18}F-4FMFES PET procedure was paired and compared with ^{18}F-FDG PET within a 2-wk interval to evaluate their complementarity for this new indication.

Hence, this report shows the preliminary trends and observations of a phase II clinical trial evaluating ^{18}F-4FMFES and ^{18}F-FDG PET in an endometrial cancer cohort. In parallel, we investigated the impact of using drugs to slow intestinal transit in combination with diuretics, as the hepatobiliary and urinary metabolites of ^{18}F-4FMFES generate an intense lower-abdomen background signal that could impair endometrial cancer assessment.

MATERIALS AND METHODS

The study was approved by the Sherbrooke University Hospital clinical research ethics committee and institutional board, performed under the authority of Health Canada and registered on ClinicalTrials.gov with the identifier NCT04823065. All patients signed an informed consent form, and the procedure was explained in lay terms by the investigators. Eligible patients were recruited after biopsy and as recommended by the gynecologic oncologists. Eligibility criteria included patients with newly diagnosed endometrial cancer, with a positive ERα status histologically confirmed. Exclusion criteria included pregnancy and concomitant endocrine therapy. In this ongoing study aiming to recruit 72 patients with ovarian and uterine cancers of various origins, the first 25 endometrial cancer patients recruited were examined using both ^{18}F-FDG and ^{18}F-4FMFES PET, as planned. Among them, 23 patients had ER+ endometrial carcinoma (including 16 who had the endometroid endometrial adenocarcinoma subtype), and 2 were diagnosed with endometrial intraepithelial neoplasia. Four of those patients were premenopausal, and 21 patients were postmenopausal. The gynecologic oncology team staged the patients according to the postsurgery pathology report. Table 1 summarizes the patient characteristics in more detail.

Radiochemistry

^{18}F was prepared by the ^{18}O(p,n)^{18}F reaction on ^{18}O-enriched water as target material using the TR-19 or TR-24 cyclotron (Advanced Cyclotron Systems, Inc.) of the Sherbrooke Molecular Imaging Center. ^{18}F-4FMFES precursor synthesis (*20*); its labeling (*21*) using an optimized automated procedure (28); and its preparation, formulation, and quality control procedures (23) were as described previously. Apparent molar activity for ^{18}F-4FMFES ranged from 20 to 123 GBq/μmol and was similar to what has been reported in the literature (*23,24*).

Pharmacologic Interventions to Slow Intestinal Transit

Patients were not allowed to drink from the time the ^{18}F-4FMFES was injected until the end of the imaging procedure. In addition, for ^{18}F-4FMFES examinations, patients received either 4 mg of loperamide orally 15 min before injection (n = 12) or 20 mg of the anticholinergic drug hyoscine *N*-butylbromide intravenously at 0, 20, and 40 min after tracer administration (n = 11). Two patients received no additional intervention and were pooled with the ^{18}F-4FMFES PET scans previously performed on breast cancer patients (n = 31) for the intestinal transit assessment analysis (*23*).

PET Imaging

A catheter was placed in the arm, and patients were injected intravenously with 210.6 ± 20.5 MBq of ^{18}F-4FMFES in a total volume of 10 mL of physiologic saline (0.9% NaCl). Thereafter, the line was flushed with 20 mL of saline. Within less than 2 wk, the same patients were injected with 320.3 ± 102.7 MBq of ^{18}F-FDG. The scans occurred in random order. For both imaging procedures, patients were injected with 40 mg of the diuretic furosemide shortly after tracer injection to clear the tracer via the urine.

All acquisitions were performed using a Discovery MI PET scanner (GE Healthcare) from mid thigh to vertex, including the upper limbs. One hour after injection, a low-dose CT acquisition was initiated, followed immediately by a PET acquisition (3–5 overlapping bed positions, 2 min each). All PET images were reconstructed using a 3-dimensional time-of-flight weighted line-of-response row-action maximum-likelihood algorithm, with attenuation correction derived from the CT attenuation map. The accuracy of the absolute count calibration of the scanner was validated against a uniform phantom containing ^{18}F at a known concentration. The measured activity was expressed as SUV for each voxel.

Image Analysis

Images were visualized and analyzed using MIM software, version 6.0 (MIM Software Inc.). Images were qualitatively evaluated with a focus on the apparent extent of the lower-abdomen background uptake emanating from the intestinal radioactive content by a nuclear medicine specialist. A region of interest (ROI) covering the whole abdomen and excluding the liver, bladder, and uterus was drawn. An arbitrary SUV threshold of more than 4, corresponding to a background value for which 80% of primary tumors observed during this study would be undetected or equivocal with 4FMFES PET, was applied to the ROI, and the volume of the resulting contour was extracted.

A volumetric ROI was drawn on each detectable tumor focus, and ROIs were also drawn in the area surrounding tumors (tumor background). The maximum-intensity voxel (SUV_{max}) was taken for tumor and uterine ROI quantification, whereas the averaged value of the voxels included in the ROIs (SUV_{mean}) was used for background regions. Tumor contrast was evaluated by the ratio of tumor uptake to its proximal background (T/B). Tumors with a T/B of less than 3.0 were considered equivocal.

Statistical Analysis

Data were reported as mean ± SD for patient numbers of 3 or more or as mean only for patient numbers of less than 3. Statistical analyses were performed using Prism software, version 7.0.4 (GraphPad Software Inc.). One-way ANOVA using the Tukey method for multiple comparisons was applied to compare ^{18}F-4FMFES and ^{18}F-FDG uptake, ^{18}F-FDG/^{18}F-4FMFES uptake ratio, and T/Bs in tumors. The threshold for significance was set a priori to a P value of less than 0.05 for each compared group.

RESULTS

Drug-Induced Intestinal ^{18}F-4FMFES Slowdown

As was observed in the past with breast cancer patients (*23,24*), the natural elimination pathway of ^{18}F-4FMFES generated extensive abdominal contamination without any additional intervention (Fig. 1A). Both the use of 4 mg of loperamide 5 min before ^{18}F-4FMFES injection and the use of repeated injection of 20 mg of hyoscine

TABLE 1
Patient Characteristics

Parameter	Data
Patients (*n*)	25
Mean age ± SD (y)	63.4 ± 10.5 (median, 66; range, 41–79)
Premenopausal (*n*)	4
Postmenopausal (*n*)	21
Histology (*n*)	
Endometrial carcinoma	23
Endometrial intraepithelial neoplasia	2
Grade (*n*)	
1	5
2	12
3	8
Treatment (*n*)	
Loperamide (4 mg)	12
Hyoscine *N*-butylbromide (3 × 20 mg)	11
None	2 (plus 31 breast cancer patients (*23*))

N-butylbromide at 0, 20, and 40 min after ^{18}F-4FMFES injection appeared to be successful to slow progression of the radioactive intestinal bolus. The use of the diuretic furosemide along with ^{18}F-4FMFES injection reduced the bladder volume and uptake in most patients. Together, the combination of furosemide and hyoscine *N*-butylbromide improved the diagnostic quality of ^{18}F-4FMFES PET for endometrial cancers (Fig. 1A).

Application of an SUV threshold of more than 4 on an abdominal ROI allowed standardized estimation of the intestinal volume containing significant contamination with ^{18}F-4FMFES radiometabolites (Fig. 1B). In the absence of intervention, the measured volume reached 1,117.8 ± 413.4 mL, which was significantly reduced by the administration of either loperamide (677.9 ± 471.2 mL; $P < 0.01$) or hyoscine *N*-butylbromide (495.7 ± 341.9 mL; $P < 0.001$). However, the background ^{18}F-4FMFES uptake in the immediate vicinity of the primary endometrial tumor was not significantly different between the control (SUV_{mean}, 0.66 ± 0.12), loperamide (SUV_{mean}, 0.58 ± 0.13), and hyoscine *N*-butylbromide (SUV_{mean}, 0.63 ± 0.15) groups.

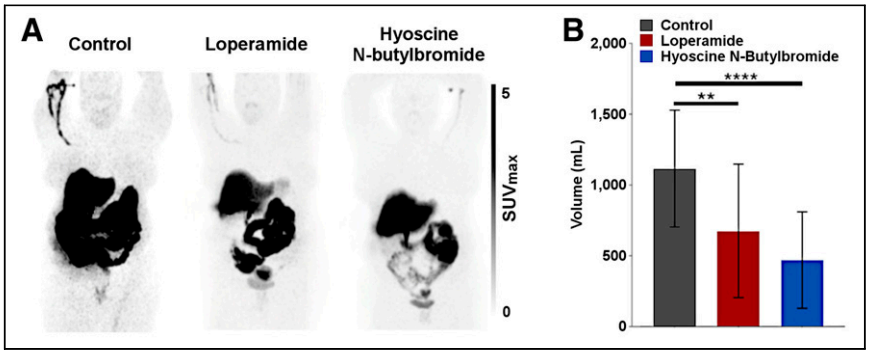

FIGURE 1. (A) Qualitative maximum-intensity-projection whole-body assessment of effect of pharmacologic interventions to slow progression of radioactive intestinal bolus. Without use of any intervention (left panel), ^{18}F-4FMFES PET typically produces intense abdominal uptake caused by progression of radiometabolites excreted by gallbladder in intestines. Ingestion of 4 mg of loperamide 15 min before injection of radiotracer yielded mitigated results (center panel). Repeated intravenous injection of 20 mg of hyoscine *N*-butylbromide at 0, 20, and 40 min after ^{18}F-4FMFES injection apparently reduced lower-abdomen background and slowed transit of radioactive intestinal bolus (right panel). (B) Measured volume extracted from application of SUV threshold of >4 on abdominal ROI. Both use of loperamide and use of hyoscine *N*-butylbromide significantly reduced intestinal background volume. $^{**}P < 0.01$. $^{****}P < 0.001$.

PET Image Qualitative Assessment

Both ^{18}F-FDG and ^{18}F-4FMFES PET were able to produce high-contrast visualization of endometrial carcinoma (Fig. 2). Two patients had sentinel node involvement, with sizes ranging from 2 to 5 mm in diameter according to pathology and lymphoscintigraphy. Those tumors could not be detected by PET imaging with either tracer and were considered within the reference range by CT. One patient had an endometroid endometrial adenocarcinoma that was detectable only using ^{18}F-4FMFES PET; the ^{18}F-FDG PET examination had negative results (Fig. 3). Pathologic examination of the surgical specimen confirmed the presence of a 2-cm grade 1 endometroid tumor. Two patients yielded a ubiquitous ^{18}F-FDG uptake (T/B, 1.9 and 2.2, respectively) that was clearly detected using ^{18}F-4FMFES PET (SUV_{max}, 11.1 and 8.5, respectively; T/B, 19.9 and 18.9, respectively). Two other patients harbored subcentimeter endometrial intraepithelial neoplasia tumors, both of which were better visualized using ^{18}F-4FMFES (average SUV_{max}, 5.7; T/B, 11.7) than ^{18}F-FDG (average SUV_{max}, 3,1; T/B, 4.8).

In 1 patient, ^{18}F-FDG PET spotted an inguinal node focus (SUV_{max}, 5.2; T/B, 7.2) that was ^{18}F-4FMFES–negative, but control ^{18}F-FDG PET/CT at a later time showed reduced uptake and a stable size reminiscent of a benign node (Fig. 4). ^{18}F-FDG PET was thus considered false-positive for this node assessment. Another patient had an ^{18}F-4FMFES–positive (SUV_{max}, 3.0; T/B, 5.0), ^{18}F-FDG–negative right iliac sentinel node (Fig. 5). Ten nodes were dissected at surgery (including the suspected one); all were negative on pathologic examination, and a control ^{18}F-FDG PET examination at 9 mo after the initial assessment showed no abnormal uptake at this site, indicating a false-positive result for ^{18}F-4FMFES for this patient.

Semiquantitative Assessment

Average endometrial tumor uptake on ^{18}F-4FMFES PET (SUV_{max}, 9.4 ± 3.2; range, 3.0–14.4) was slightly higher than on ^{18}F-FDG PET (SUV_{max}, 7.5 ± 5.1; range, 0–22.0), but the difference was not significant. Uptake did not significantly differ between endometroid tumors and endometrial carcinomas with either tracer (Fig. 6A). ^{18}F-FDG uptake followed a continuous increase according to grade, with a significant difference between grade 1 tumors (SUV_{max}, 4.0 ± 2.0) and grade 2 tumors (SUV_{max}, 8.0 ± 4.9; $P < 0.05$) and between grade 1 tumors and grade 3 tumors (SUV_{max}, 9.7 ± 3.0; $P < 0.01$). ^{18}F-4FMFES uptake peaked in grade 2 tumors at an SUV_{max} of 11.4 ± 2.3, which was significantly higher than in grade 1 tumors (SUV_{max}, 6.9 ± 2.6; $P < 0.05$) but was not significantly different from grade 3 tumors (SUV_{max}, 9.2 ± 3.1; $P = 0.53$) (Fig. 6A).

Contrast values, as defined by T/Bs, were 2.3-fold higher ($P < 0.0001$) for ^{18}F-4FMFES than for ^{18}F-FDG (16.9 ± 6.3 and 7.4 ± 4.6,

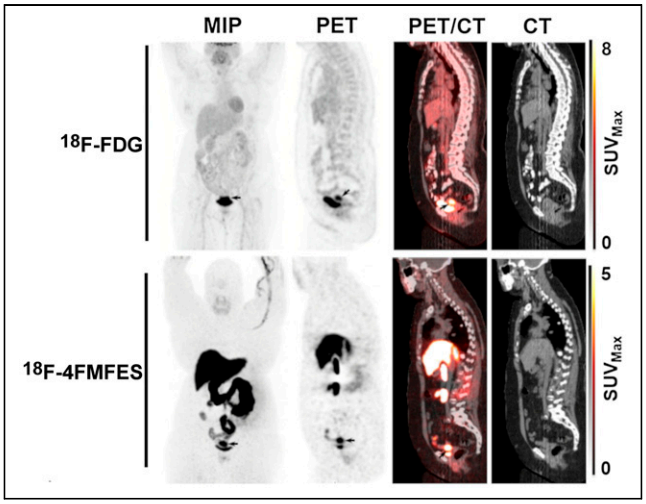

FIGURE 2. Representative case of endometrial carcinoma (arrows) imaged with ^{18}F-FDG PET/CT (top row) and ^{18}F-4FMFES PET/CT (bottom row), displayed in frontal maximum-intensity projection (MIP) and in sagittal views.

respectively). T/Bs significantly differed between grade 1 tumors (10.5 ± 3.8) and grade 2 tumors (18.0 ± 4.4; $P < 0.01$) and grade 3 tumors (17.5 ± 5.6; $P < 0.05$) using ^{18}F-4FMFES PET (Fig. 6B). Such T/B relationships according to grade were not found for ^{18}F-FDG PET (Fig. 6B), as the slight differences observed were not significantly different.

The ^{18}F-FDG/^{18}F-4FMFES uptake ratio was also measured according to grade (Fig. 6C), similarly to previous publications (*13–15,17*). Although the ^{18}F-FDG/^{18}F-4FMFES ratio was similar between grade 1 and 2 tumors (0.65 ± 0.35 and 0.77 ± 0.40, respectively), a significant increase ($P < 0.05$) over grade 1 was observed for grade 3 tumors, with a value of 1.25 ± 0.64.

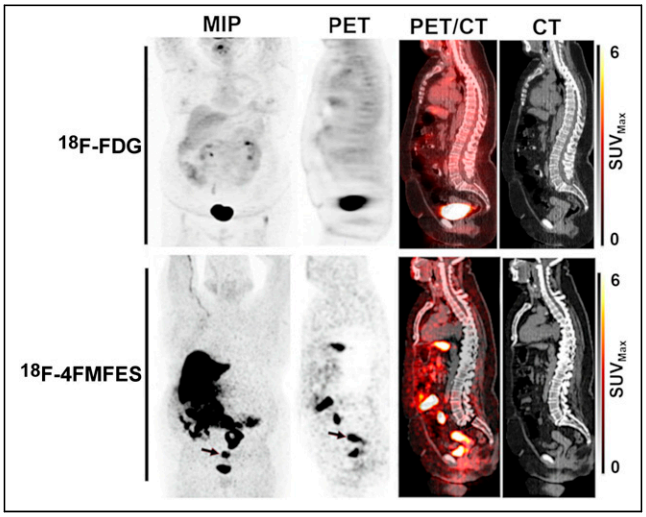

FIGURE 3. A 69-y-old endometroid adenocarcinoma patient with ^{18}F-FDG–negative, ^{18}F-4FMFES–positive primary tumor. ^{18}F-FDG PET did not yield any abnormal uptake in uterus, whereas ^{18}F-4FMFES PET revealed intense signal (SUV_{max}, 9.6; arrows) over 44 × 32 × 25 mm region. Postsurgery pathology report measured size of tumor to be 20 mm in its long axis, meaning ^{18}F-4FMFES overestimated size of tumor in this case.

DISCUSSION

In this preliminary assessment, the use of combined ^{18}F-FDG and ^{18}F-4FMFES PET imaging was investigated in recently diagnosed ER+ endometrial cancer patients. At first, the application of interventions aiming to slow progression of the radioactive intestinal bolus after ^{18}F-4FMFES injection to improve image quality in the abdomen produced variable results. Baseline ^{18}F-4FMFES image quality in the abdominal region was relatively poor because of the abundant presence of radioactive intestinal content. Predosing with loperamide, a peripheral opioid used mainly for control of diarrhea, moderately reduced the distribution of the abdominal contamination. Increasing the dosage of loperamide might yield better results, at the cost of the associated discomfort of prolonged constipation for the patient. In contrast, repeated injection of hyoscine *N*-butylbromide during tracer administration, a routine procedure for radiologic assessment of the intestines, substantially slowed transit of the intestinal content and improved overall abdominal ^{18}F-4FMFES image quality in assessed patients. Even if the PET/CT assessment of anatomic planes usually allows distinction between the uterus and the intestines, and even if the pharmacologic interventions do not impact the uterine region background, such an intervention might be useful for nonambiguous diagnosis of locoregional metastases using ^{18}F-4FMFES PET in advanced-stage patients.

Although both tracers yielded similar uptake overall in endometrial tumors, detectability was noticeably improved using ^{18}F-4FMFES over

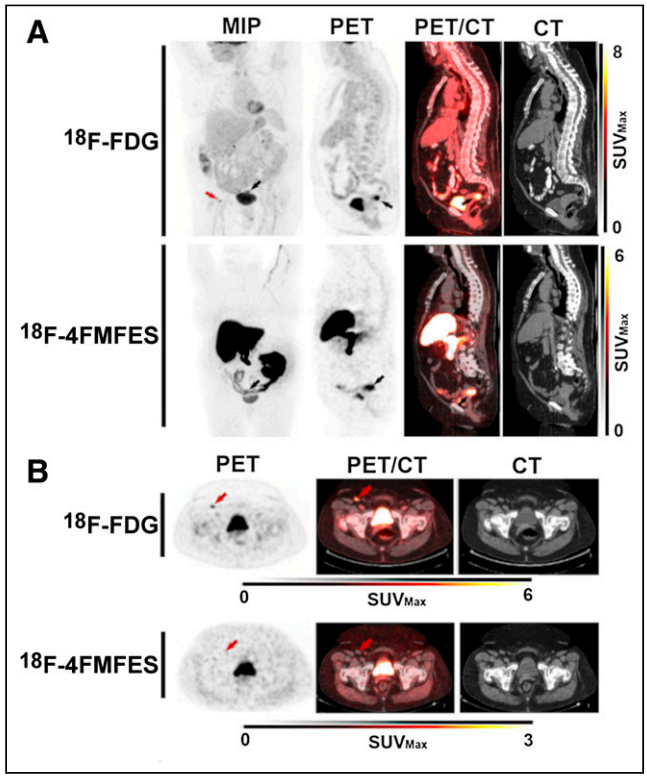

FIGURE 4. A 75-y-old endometroid adenocarcinoma patient with ^{18}F-FDG false-positive inguinal node. (A) Endometroid adenocarcinoma primary tumor, with SUV_{max} uptake of 12.3 for ^{18}F-FDG and 8.9 for ^{18}F-4FMFES (black arrows). The ^{18}F-FDG PET also revealed a suspected right inguinal node metastasis (red arrow), which yielded SUV_{max} of 5.2 (T/B, 7.2). (B) Transaxial slices of the suspected inguinal node metastasis (red arrows). The ^{18}F-FDG–positive node was ^{18}F-4FMFES–negative and of normal appearance in CT image. Pathology examination considered inguinal node as normal, meaning ^{18}F-FDG signal was false-positive.

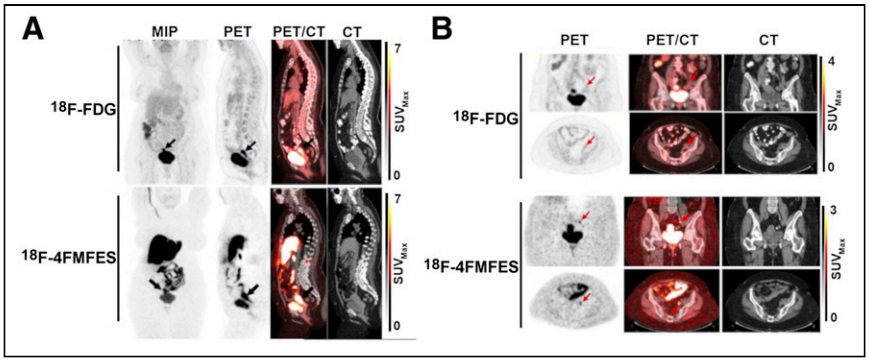

FIGURE 5. A 67-y-old endometrial carcinoma patient with ^{18}F-4FMFES false-positive iliac node. (A) Endometrial carcinoma primary tumor, with SUV_{max} uptake of 12.9 for ^{18}F-FDG and 12.7 for ^{18}F-4FMFES (arrows). (B) Coronal (top) and transaxial (bottom) views centered on suspected left iliac sentinel node metastasis with ^{18}F-4FMFES (arrows), which was of normal aspect in CT images. Pathology examination after surgery considered iliac node normal, confirming false-positive result for ^{18}F-4FMFES.

^{18}F-FDG, as measured by the increased T/B obtained. As a result, all primary tumors assessed were clearly visualized using ^{18}F-4FMFES PET, whereas 2 patients obtained a ubiquitous signal (T/B < 3) at the tumor site using ^{18}F-FDG PET. Moreover, 1 patient was ^{18}F-FDG–negative and ^{18}F-4FMFES+, with CT and surgical-sample examination instead showing the presence of a 20-mm tumor and confirming a false-negative result for ^{18}F-FDG. One patient presented with suspected sentinel node uptake on ^{18}F-FDG PET that was negative on ^{18}F-4FMFES PET, but its subsequent biopsy invalidated the presence of cancer in the assessed tissue, meaning a false-positive result for ^{18}F-FDG. Only 1 confirmed false-positive case was found for ^{18}F-4FMFES PET, in which a node with substantial ^{18}F-4FMFES uptake (and ^{18}F-FDG–negative) was exempt from cancer cells in the pathologic examination. Although anecdotal, those few examples in our relatively modest sample size might suggest a better overall sensitivity and specificity for ^{18}F-4FMFES over ^{18}F-FDG in ER+ endometrial cancers, as well as a good complementarity between the 2 tracers.

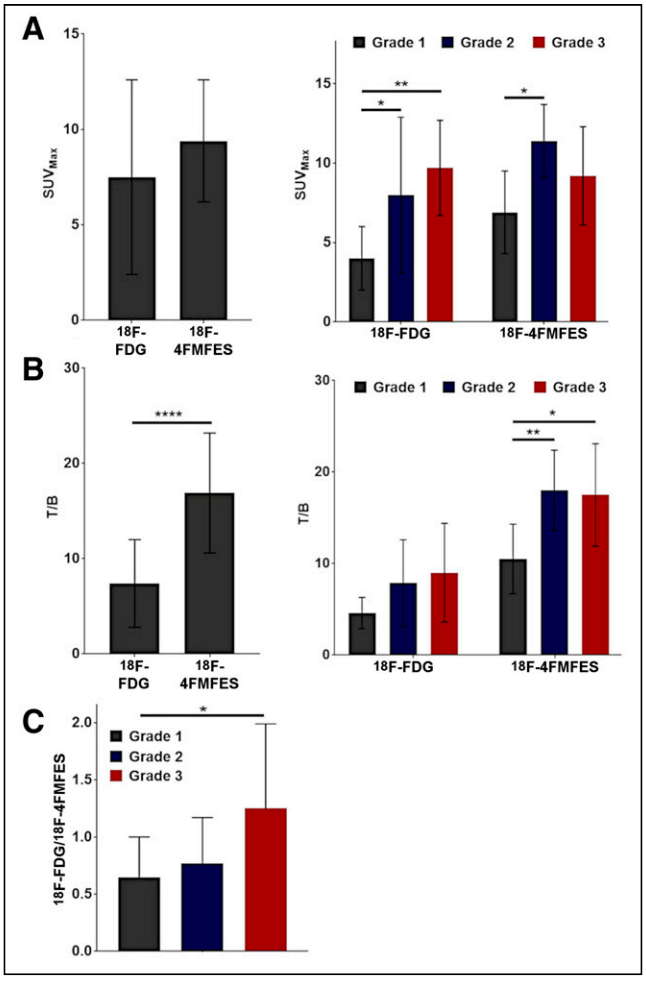

FIGURE 6. Semiquantitative ^{18}F-FDG and ^{18}F-4FMFES uptake and T/Bs. (A) ^{18}F-FDG and ^{18}F-4FMFES uptake (SUV_{max}) for whole sample (left) and according to grade (right) (B) ^{18}F-FDG and ^{18}F-4FMFES T/Bs for whole studied sample (left) and according to grade (right). (C) ^{18}F-FDG and ^{18}F-4FMFES T/Bs according to grade. *$P < 0.05$. **$P < 0.01$. ****$P < 0.001$.

The 2 cases of endometrial interepithelial neoplasia observed so far in our study showed a slightly higher uptake for ^{18}F-4FMFES than for ^{18}F-FDG, along with a 2.4-fold higher T/B, and as such it could be interesting to investigate further the use of ^{18}F-4FMFES PET for this hard-to-detect small-sized subclass of endometrial tumor. Of equal interest would be other less frequent uterine cancers that were previously investigated with ^{18}F-FES PET, including ER+ mesenchymal (*13*) and sarcoma (*15*) tumors, and our group will actively seek to recruit patients harboring those subtypes during the ongoing trial.

A significantly higher tumor uptake of ^{18}F-4FMFES was observed for grade 1 tumors than for grade 2 tumors, whereas ^{18}F-FDG PET uptake was significantly different between grade 1 and grade 2 and 3 tumors. This trend contradicts a previously published result showing that grade 1 cancers yielded significantly higher ^{18}F-FES uptake than higher-grade tumors (*12*)—a result that will need to be further investigated. T/Bs for ^{18}F-FDG were unable to discern between grades. In contrast, ^{18}F-4FMFES T/Bs were able to properly differentiate low-grade tumors from grade 2 and 3 tumors. As such, both ^{18}F-4FMFES uptake and T/Bs can be useful to distinguish between low- and high-grade endometrial tumors.

The ^{18}F-FDG/^{18}F-4FMFES uptake ratio was also measured. A significantly higher ^{18}F-FDG/^{18}F-4FMFES ratio was measured for grade 3 than for grade 1 tumors, similar to what was previously observed for the ^{18}F-FDG/^{18}F-FES ratio in endometrial cancers (*12,14,15,17*). A higher ^{18}F-FDG/^{18}F-FES ratio also correlated with worse progression-free and overall survival (*17*). As such, the ^{18}F-FDG/^{18}F-4FMFES ratio could equal the usefulness of the previously evaluated ^{18}F-FDG/^{18}F-FES ratio in differentiating tumors of different grades or patient outcomes.

So far, all recruited patients have been newly diagnosed and at an early stage, thus disabling any comparison of ^{18}F-FDG and ^{18}F-4FMFES according to stage. In view of a previous study (*12*) in which a nonsignificant trend toward lower ^{18}F-FES uptake and higher ^{18}F-FDG uptake was observed for advanced endometrial cancers, the same tendency is expected using the similar ^{18}F-4FMFES tracer. A related drawback of this low-stage patient sample is the lack of metastatic disease in this study. Although the assessment of primary tumors with ^{18}F-4FMFES PET was an essential first step in evaluating the endometrial tumor–targeting properties of the tracer, PET imaging procedures are expected to reach their full usefulness on patients with

disseminated diseases that are more challenging to adequately assess using standard procedures. Further studies will be needed to evaluate ^{18}F-4FMFES PET in advanced endometrial cancer.

CONCLUSION

It is possible to lessen ^{18}F-4FMFES abdominal background uptake using hyoscine *N*-butylbromide. Both ^{18}F-FDG and ^{18}F-4FMFES PET are suitable for detection of ER+ endometrial cancers, although tumor contrast is better with ^{18}F-4FMFES than with ^{18}F-FDG.

DISCLOSURE

This work was supported through the Innovation Grant program of the Canadian Cancer Society Research Institute (grant 705984), with support from the Ann Matyas Cancer Research Fund. No other potential conflict of interest relevant to this article was reported.

ACKNOWLEDGMENTS

We thank Stéphanie Dubreuil for her contribution to the clinical protocol revision and ^{18}F-4FMFES pharmacovigilance. We also thank the nuclear medicine and cyclotron staff from our facility that indirectly supported the project.

KEY POINTS

QUESTION: Will ^{18}F-4FMFES PET, along with pharmaceutic interventions to reduce abdominal background uptake, improve the detection of ER+ endometrial cancers and allow grade segmentation in combination with ^{18}F-FDG PET?

PERTINENT FINDINGS: The use of hyoscine *N*-butylbromide in repeated intravenous injection significantly reduced the extent of the abdominal background uptake resulting from the natural elimination of ^{18}F-4FMFES. ^{18}F-4FMFES PET yielded better tumor contrast than did ^{18}F-FDG PET in ER+ endometrial cancers. Both tracers succeeded in distinguishing between low- and high-grade cancers.

IMPLICATIONS FOR PATIENT CARE: Because of the high tumor contrast it displays, ^{18}F-4FMFES PET in combination with repeated injection of hyoscine *N*-butylbromide may improve the locoregional and whole-body assessment of advanced ER+ endometrial cancers, compared with ^{18}F-FDG PET.

REFERENCES

1. Bray F, Ferlay J, Soerjomataram I, Siegel RL, Torre LA, Jemal A. Global cancer statistics 2018: GLOBOCAN estimates of incidence and mortality worldwide for 36 cancers in 185 countries. *CA Cancer J Clin.* 2018;68:394–424.
2. Köbel M, Atenafu EG, Rambau PF, et al. Progesterone receptor expression is associated with longer overall survival within high-grade histotypes of endometrial carcinoma: a Canadian high-risk endometrial cancer consortium (CHREC) study. *Gynecol Oncol.* 2016;141:559–563.
3. Vahrenkamp JM, Yang CH, Rodriguez AC, et al. Clinical and genomic crosstalk between glucocorticoid receptor and estrogen receptor α in endometrial cancer. *Cell Rep.* 2018;22:2995–3005.
4. Tomica D, Rami S, Danoli D, Šušnjar L, Peri-Balja M, Puljiz M. Impact of oestrogen and progesterone receptor expression in the cancer cells and myometrium on survival of patients with endometrial cancer. *J Obstet Gynaecol.* 2018;38:96–102.
5. Zhang Y, Zhao D, Gong C, et al. Prognostic role of hormone receptors in endometrial cancer: a systematic review and meta-analysis. *World J Surg Oncol.* 2015;13:208.
6. Thigpen T, Brady MF, Homesley HD, Soper JT, Bell J. Tamoxifen in the treatment of advanced or recurrent endometrial carcinoma: a Gynecologic Oncology Group study. *J Clin Oncol.* 2001;19:364–367.
7. Rieber A, Nussle K, Stohr I, et al. Preoperative diagnosis of ovarian tumors with MR imaging: comparison with transvaginal sonography, positron emission tomography, and histologic findings. *AJR.* 2001;177:123–129.
8. Kakhki VR, Shahriari S, Treglia G, et al. Diagnostic performance of fluorine-18 fluorodeoxyglucose positron emission tomography imaging for detection of primary lesion and staging of endometrial cancer patients: systematic review and metaanalysis of the literature. *Int J Gynecol Cancer.* 2013;23:1536–1543.
9. Narayanan P, Sahdev A. The role of ^{18}F-FDG PET CT in common gynaecological malignancies. *Br J Radiol.* 2017;90:20170283.
10. Yu JQ, Doss M, Alpaugh RK. Normal variants and pitfalls encountered in PET assessment of gynecologic malignancies. *PET Clin.* 2018;13:249–268.
11. Lakhani A, Khan SR, Bharwani N, et al. FDG PET/CT pitfalls in gynecologic and genitourinary oncologic imaging. *Radiographics.* 2017;37:577–594.
12. Tsujikawa T, Yoshida Y, Kiyono Y, et al. Functional oestrogen receptor α imaging in endometrial carcinoma using 16α-[^{18}F]fluoro-17β-oestradiol PET. *Eur J Nucl Med Mol Imaging.* 2011;38:37–45.
13. Zhao Z, Yoshida Y, Kurokawa T, Kiyono Y, Mori T, Okazawa H. ^{18}F-FES and ^{18}F-FDG PET for differential diagnosis and quantitative evaluation of mesenchymal uterine tumors: correlation with immunohistochemical analysis. *J Nucl Med.* 2013;54:499–506.
14. Tsujikawa T, Yoshida Y, Mori T, et al. Uterine tumors: pathophysiologic imaging with 16α-[^{18}F]fluoro-17β-estradiol and ^{18}F fluorodeoxyglucose PET: initial experience. *Radiology.* 2008;248:599–605.
15. Yamamoto M, Tsujikawa T, Yamada S, et al. ^{18}F-FDG/^{18}F-FES standardized uptake value ratio determined using PET predicts prognosis in uterine sarcoma. *Oncotarget.* 2017;8:22581–22589.
16. van Kruchten M, Hospers GA, Glaudemans AW, Hollema H, Arts HJ, Reyners AK. Positron emission tomography imaging of oestrogen receptor-expression in endometrial stromal sarcoma supports oestrogen receptor-targeted therapy: case report and review of the literature. *Eur J Cancer.* 2013;49:3850–3855.
17. Yamada S, Tsuyoshi H, Yamamoto M, et al. Prognostic value of 16α-^{18}F-fluoro-17β-estradiol PET as a predictor of disease outcome in endometrial cancer: a prospective study. *J Nucl Med.* 2021;62:636–642.
18. Mankoff DA, Tewson TJ, Eary JF. Analysis of blood clearance and labeled metabolites for the estrogen receptor tracer [F-18]-15α-fluorestradiol (FES). *Nucl Med Biol.* 1997;24:341–348.
19. Tewson TJ, Mankoff DA, Peterson LM, Woo I, Petra P. Interactions of 16α-[^{18}F]-fluoroestradiol (FES) with sex steroid binding protein (SBP). *Nucl Med Biol.* 1999; 26:905–913.
20. Seimbille Y, Ali H, van Lier JE. Synthesis of 2,16α- and 4,16α-difluoroestradiols and their 11β-methoxy derivatives as potential estrogen receptor-binding radiopharmaceuticals. *J Chem Soc Perkin Trans.* 2002;1:657–663.
21. Seimbille Y, Rousseau J, Bénard F, et al. ^{18}F-labeled difluoroestradiols: preparation and preclinical evaluation as estrogen receptor-binding radiopharmaceuticals. *Steroids.* 2002;67:765–775.
22. Beauregard JM, Croteau E, Ahmed N, van Lier JE, Bénard F. Assessment of human biodistribution and dosimetry of 4-fluoro-11β-methoxy-16α-^{18}F-fluoroestradiol using serial whole-body PET/CT. *J Nucl Med.* 2009;50:100–107.
23. Paquette M, Lavallée É, Phoenix S, et al. Improved estrogen receptor assessment by PET using the novel radiotracer 4FMFES in ER+ breast cancer patients: an ongoing phase II clinical trial. *J Nucl Med.* 2018;59:197–203.
24. Paquette M, Lavallée É, Phoenix S, et al. Combined FDG and 4FMFES PET imaging in ER+ breast cancer patients for improved diagnostic and prognostic value [abstract]. *Eur J Nucl Med Mol Imaging.* 2017;44(suppl 2):OP-302.
25. Groheux D, Giacchetti S, Moretti JL, et al. Correlation of high ^{18}F-FDG uptake to clinical, pathological and biological prognostic factors in breast cancer. *Eur J Nucl Med Mol Imaging.* 2011;38:426–435.
26. Koo HR, Park JS, Kang KW, et al. ^{18}F-FDG uptake in breast cancer correlates with immunohistochemically defined subtypes. *Eur Radiol.* 2014;24:610–618.
27. Kurland BF, Peterson LM, Lee JH, et al. Estrogen receptor binding (FES PET) and glycolytic activity (FDG PET) predict progression-free survival on endocrine therapy in patients with ER+ breast cancer. *Clin Cancer Res.* 2017;23:407–415.
28. Ahmed N, Langlois R, Rodrigue S, Benard F, van Lier JE. Automated synthesis of 11β-methoxy-4,16α-[16α-^{18}F]difluoroestradiol (4F-M[^{18}F]FES) for estrogen receptor imaging by positron emission tomography. *Nucl Med Biol.* 2007;34:459–464.